Thermoelectric Properties and Site-Selective Rb^+/K^+ Distribution in the $K_{2-x}Rb_xBi_8Se_{13}$ Series

Theodora Kyratsi,[†] Duck-Young Chung,[†] John R. Ireland,[‡] Carl R. Kannewurf,[‡] and Mercouri G. Kanatzidis*,[†]

Department of Chemistry, Michigan State University, East Lansing, Michigan 48824, and Department of Electrical and Computer Engineering, Northwestern University, Evanston, Illinois 60208

Received March 21, 2003. Revised Manuscript Received May 6, 2003

β-$K_2Bi_8Se_{13}$ possesses promising thermoelectric properties whereas $Rb_2Bi_8Se_{13}$ does not. The formation of solid solutions between these two compounds was attempted to study the alkali metal distribution in the structure and its influence in the electronic properties. The structure of the $K_{2-x}Rb_xBi_8Se_{13}$ series of solid solutions was studied and the members with $0 < x \leq 1$ were found to adopt the β-$K_2Bi_8Se_{13}$ structure. Detailed crystallographic studies were performed for the $x = 1.0$ composition to examine in detail the K/Rb distribution in the lattice and the effect on the K/Bi disorder that exists in the β-$K_2Bi_8Se_{13}$ structure. The Rb^+ ions occupy exclusively one crystallographic site replacing K^+. This defines $RbKBi_8Se_{13}$ as a new quaternary compound. Lattice parameters and band gaps are reported for the different compositions. Charge transport measurements including electrical conductivity, thermoelectric power, and Hall effect show that the materials are n-type semiconductors with increasing carrier concentration as a function of composition x.

Introduction

β-$K_2Bi_8Se_{13}$[1] is a promising material among many ternary and quaternary compounds of the bismuth chalcogenides[2] that were investigated for thermoelectric applications. It has a complex monoclinic crystal structure that includes two different interconnected types of Bi/Se building blocks (the so-called $NaCl^{100}$- and $NaCl^{111}$-type) and K^+ atoms in tunnels. The two different Bi/Se blocks are connected to each other at special mixed-occupancy K/Bi sites that seem to be crucial in defining the electronic structure near the Fermi level and the electronic properties.[3] Depending on doping, β-$K_2Bi_8Se_{13}$ can possess a relatively high power factor ($S^2\sigma$) and a promising ZT.[4,5]

Solid solutions based on the β-$K_2Bi_8Se_{13}$ structure were successfully prepared via substitution on the heavy metal sites (i.e., $K_2Bi_{8-x}Sb_xSe_{13}$)[6] and on the chalcogenide sites (i.e., $K_2Bi_8Se_{13-x}S_x$).[7] Because $K_2Sb_8Se_{13}$ and $K_2Bi_8S_{13}$ are isostructural to β-$K_2Bi_8Se_{13}$ the full range in composition was possible, however, there are no isostructural analogues with different alkali metals. With Rb and Cs the compound forms with the same composition $A_2Bi_8Se_{13}$ (A:Rb, Cs) but that forms a different structure type.[8] The study of the $K_2Bi_{8-x}Sb_xSe_{13}$ solid solutions[6] showed that the Bi/Sb distribution in the metal sites was nonuniform[9] at low x values. By contrast, in $K_2Bi_8Se_{13-x}S_x$[7] the Se/S distribution was more even, indicating the formation of more homogeneous solid solutions.

In this work we explore the $K_{2-x}Rb_xBi_8Se_{13}$ series to determine the limits of the K/Rb ratio between two different structure types. We also attempt to specify which K sites are particularly amenable to Rb substitution in $K_2Bi_8Se_{13}$. This is an important issue because the content of these sites affects the electrical properties of the material. Lattice parameters and semiconducting band gaps are reported as a function of composition. The charge transport properties including electrical conductivity, thermoelectric power, and Hall effect were studied as a function of temperature to assess the potential of these materials as good thermoelectrics.

Experimental Section

Reagents. High-purity (99.999%) bismuth and selenium used in this work were generously provided by Tellurex Inc. (Traverse City, MI). Potassium chunks (98%, Aldrich Chemical

* To whom correspondence should be addressed.
[†] Michigan State University.
[‡] Northwestern University.

(1) Chung, D.-Y.; Choi, K.-S.; Iordanidis, L.; Schindler, J. L.; Brazis, P. M.; Kannewurf, C. R.; Chen, B.; Hu, S.; Uher, C.; Kanatzidis, M. G. *Chem. Mater.* **1997**, *9* (12), 3060.

(2) (a) Kanatzidis, M. G. *Semiconductors Semimetals* **2000**, *69*, 51. (b) Chung, D.-Y.; Iordanidis, L.; Choi, K.-S.; Kanatzidis, M. G. *Bull. Kor. Chem. Soc.* **1998**, *19*, 1283.

(3) Bilc, D.; Mahanti, S. D.; Larson, P.; Kanatzidis, M. G., submitted to *Phys. Rev. B*.

(4) $ZT = (S^2\sigma/\kappa)T$, where σ is the electrical conductivity, S is the Seebeck coefficient, κ is the thermal conductivity, and T is the temperature. The factor $S^2\sigma$ is called the power factor.

(5) Brazis, P. W.; Rocci-Lane, M.; Ireland, J. R.; Chung, D.-Y.; Kanatzidis, M. G.; Kannewurf, C. R. *Proceedings of the 18th International Conference on Thermoelectrics*; IEEE, Inc., 1999; p 619.

(6) Kyratsi, Th.; Dyck, J. S.; Chen, W.; Chung, D.-Y.; Uher, C.; Paraskevopoulos, K. M.; Kanatzidis, M. G. *J. Appl. Phys.* **2002**, *92* (2), 965.

(7) Kyratsi, Th.; Kanatzidis, M. G., work in progress.

(8) Iordanidis, L.; Brazis, P. W.; Kyratsi, Th.; Ireland, J.; Lane, M.; Kannewurf, C. R.; Chen, W.; Dyck, J. S.; Uher, C.; Ghelani, N.; Hogan, T.; Kanatzidis, M. G. *Chem. Mater.* **2001**, *13*, 622.

(9) Kyratsi, Th.; Chung, D.-Y.; Kanatzidis, M. G. *J. Alloys Compd.* **2002**, *338* (1−2), 36.

10.1021/cm034185v CCC: $25.00
Published on Web 06/25/2003

Co., Inc., Milwaukee, WI) and rubidium metal (99.8% purity, Alfa Aesar, Ward Hill, MA) were purchased. Rb_2Se was prepared by stoichiometric reaction of rubidium metal and selenium in liquid ammonia.

Synthesis and Crystal Growth. All manipulations were carried out under a dry nitrogen atmosphere in a Vacuum Atmospheres Dri-Lab glovebox. A mixture of potassium metal, rubidium selenide, bismuth, and selenium was loaded into a quart tube and subsequently flame-sealed at a residual pressure of $<10^{-4}$ Torr. For example, $KRbBi_8Se_{13}$ was prepared by mixing 0.042 g of K (1.1 mmol), 0.133 g of Rb_2Se (0.5 mmol), 1.7767 g of Bi (8.5 mmol), and 1.0489 g of Se (13.3 mmol). The mixture was heated to 850 °C over 12 h and kept there for 1 h, followed by cooling to 50 °C at a rate of −15 °C/h. The product was annealed at 500 °C for 48 h to have pure β-$K_2Bi_8Se_{13}$ phase.

Physicochemical Characterization. Differential thermal analysis (DTA) was performed with a computer-controlled Shimadzu DTA-50 thermal analyzer using a procedure described elsewhere.[6,8] The sample after the experiment was examined with powder X-ray diffraction to see possible phase changes.

Optical diffuse reflectance measurements were carried out on finely ground samples in the infrared region (6000−400 cm^{-1}) with the use of a Nicolet MAGNA-IR 750 spectrometer equipped with a diffuse reflectance attachment from Spectra-Tech. Inc. at room temperature. The measurement of diffuse reflectivity can be used to obtain values for the band gap[1,6,8] by using Kubelka−Munk[10]-type analysis.

dc electrical conductivity and thermopower measurements were made on small polycrystalline samples with the long dimension along the crystallographic *b*-axis. Typical sample sizes were 1.0−1.5 mm in length with the cross-sectional dimensions being on the order of 0.1 mm. Conductivity and thermoelectric power data were obtained with computer-automated systems described elsewhere.[11,12]

The solid solutions were examined by X-ray powder diffraction for phase identification, assessment of phase purity, and determination of lattice parameters. Diffraction patterns were obtained using a Rigaku Rotaflex powder X-ray diffractometer with Ni-filtered Cu Kα radiation operating at 45 kV and 100 mA. The data were collected at a rate of 1°/min. The purity of phases for the solid solutions was confirmed by comparison of the X-ray powder diffraction pattern to the calculated one from single-crystal data for β-$K_2Bi_8Se_{13}$ using Cerius^2 software.[13]

Single-Crystal X-ray Crystallography. Intensity data were collected at room temperature on a Bruker SMART Platform CCD diffractometer. The individual frames were measured with an omega rotation of 0.3° and an acquisition time of 30 s for a single crystal obtained from the $x = 1.0$ composition of $K_{2-x}Rb_xBi_8Se_{13}$. The SMART[14] software was used for the data acquisition and SAINT[15] software for data extraction and reduction. An analytical absorption correction was performed using face indexing and the program XPREP in the SAINT software package, followed by a semiempirical absorption correction based on symmetrically equivalent reflections with the program SADABS.[16] Structural solution and refinements were successfully done using the SHELXTL[17] package of crystallographic programs. The structure was solved with direct methods.

Table 1. Summary of Crystallographic Data and Structural Analysis for the Compound $KRbBi_8Se_{13}$

refined formula	$K_1Rb_1Bi_8Se_{13}$
formula weight	2826.74
crystal habit	black needle
crystal size, mm^3	$0.233 \times 0.002 \times 0.003$
space group	$P2_1/m$
a, Å	17.568(3)
b, Å	4.1924(7)
c, Å	18.499(3)
β, deg	90.383(3)
Z; *V*, $Å^3$	2; 1362.4(4)
D_{calc}, g cm^{-3}	6.890
temp, K	293(2)
λ(Mo Kα), Å	0.71073
absorption coefficient, mm^{-1}	70.824
F(000)	2327
$\theta_{min} - \theta_{max}$, deg	3.30 to 30.33
index ranges	$-24 \le h \le 23$ $-5 \le k \le 5$ $-25 \le l \le 25$
total reflections collected	15715
independent reflections	4328 [R(int) = 0.0630]
refinement method	full-matrix least-squares on F^2
data/restraints/parameters	4328/2/151
final *R* indices [$I > 2\sigma(I)$]	R1 = 0.0391, wR2 = 0.0762[a]
R indices (all data)	R1 = 0.0819, wR2 = 0.0874[a]
largest diff. peak and hole, e A^{-3}	4.468 and −3.838
goodness-of-fit on F^2	0.942

[a] $R1 = \sum||F_o| - |F_c||/\sum|F_o||$. $wR2 = \{\sum[w(F_o^2 - F_c^2)^2]/\sum[w(F_o^2)^2]\}^{1/2}$.

After successful assignment of the high electron density peaks to Bi, K, and Se atoms, the structural model was turned to be isostructural to β-$K_2Bi_8Se_{13}$. The thermal displacement parameters and occupancy factor on each atomic site were examined. All Se atom sites were fully occupied with reasonable thermal displacement parameters. The two heavy metal sites were modeled with a disorder involving both Bi and K atoms (Bi(8)/K3 and Bi(9)/K1). The K(2) site in the β-$K_2Bi_8Se_{13}$ structure was assigned to be a Rb atom with full occupancy. After successive refinements of the positions and occupancies of all atom sites, reasonable thermal parameters and occupancies were obtained, as well as low residual electron densities. Because of the multiple positional disorder in several atom sites, only Bi(1) to Bi(7) and all Se sites were anisotropically refined. The final formula was refined to $K_1Rb_1Bi_8Se_{13}$. The complete data collection parameters, details of the structure solution, and refinement for the compound are given in Table 1. The fractional coordinates and temperature factors (U_{eq}) of all the atoms with estimated standard deviations are given in Tables 2 and 3.

Results and Discussion

Synthesis, Characterization, and Thermal Analysis. The $K_{2-x}Rb_xBi_8Se_{13}$ series of compounds were prepared by reacting stoichiometric combinations of elemental K, Bi, Se, and Rb_2Se at 850 °C. Members with *x* value up to 1 adopt the β-$K_2Bi_8Se_{13}$ structure while those with $1.8 \le x \le 2$ adopt the $Rb_2Bi_8Se_{13}$ structure. For $1 < x < 1.8$ a biphasic mixture was obtained. An annealing step at 500 °C for 48 h was required for the members where $x \le 1$ to achieve phase-pure products and to avoid the $K_{2.5}Bi_{8.5}Se_{14}$-type phase[1] as an impurity. This behavior is similar to that of β-$K_2Bi_8Se_{13}$ that requires an annealing treatment to convert γ-$K_2Bi_8Se_{13}$ ($K_{2.5}Bi_{8.5}Se_{14}$-type structure) to the β-form.[18] The products have a highly oriented needlelike crystal morphol-

(10) (a) Wendlandt, W. W.; Hecht, H. G. *Reflectance Spectroscopy*; Interscience Publishers: New York, 1966. (b) Kotum, G. *Reflectance Spectroscopy*; Springer-Verlag: New York, 1969. (c) Tandon, S. P.; Gupta, J. P. *Phys. Status Solidi* **1970**, *38*, 363.

(11) Lyding, J. W.; Marcy, H.; Marks, T. J.; Kannewurf, C. R. *IEEE Trans. Instrum. Meas.* **1988**, *37*, 76.

(12) Brazis, P. W. Ph.D. Thesis, Northwestern University 2000; Dissertation Abstracts No. 9974255.

(13) *CERIUS^2, Version 2.35*; Molecular Simulations Inc.: Cambridge, U.K., 1995.

(14) *SMART: 1994*; Siemens Analytical Xray Systems, Inc.: Madison, WI, 1994.

(15) *SAINT: Version 4, 1994−1996*; Siemens Analytical Xray Systems, Inc.: Madison, WI, 1994−1996.

(16) Sheldrick, G. M. University of Göttingen, Göttingen, Germany, to be published.

(17) Sheldrick, G. M. *SHELXTL: Version 5, 1994*; Siemens Analytical Xray Systems, Inc.: Madison, WI, 1994.

(18) Kyratsi, Th.; Chung, D.-Y.; Kanatzidis, M. G., unpublished results.

Table 2. Atomic Coordinates (×10⁴), Equivalent Isotropic Displacement Parameters (Å² × 10³), and Occupancies for the Compound $KRbBi_8Se_{13}$

	x	*y*	*z*	*U*(eq)[a]	occ
Rb(2)	4796(1)	−7500	1563(1)	41(1)	1
Bi(1)	9198(1)	7500	790(1)	18(1)	1
Bi(2)	11720(1)	−2500	1238(1)	18(1)	1
Bi(3)	6739(1)	−2500	198(1)	17(1)	1
Bi(4)	8944(1)	−2500	4760(1)	23(1)	1
Bi(5)	6971(1)	−7500	4521(1)	19(1)	1
Bi(6)	10136(1)	2500	2524(1)	20(1)	1
Bi(7)	4940(1)	−12500	3896(1)	21(1)	1
Se(1)	9841(1)	2500	4047(1)	20(1)	1
Se(2)	10416(1)	2500	920(1)	15(1)	1
Se(3)	8074(1)	2500	580(1)	22(1)	1
Se(4)	3903(1)	−12500	2780(1)	23(1)	1
Se(5)	8131(1)	−7500	5565(1)	20(1)	1
Se(6)	7719(1)	−2500	3727(1)	20(1)	1
Se(7)	8981(1)	7500	2250(1)	18(1)	1
Se(8)	11306(1)	−2500	2659(1)	18(1)	1
Se(9)	6372(1)	−2500	1651(1)	25(1)	1
Se(10)	4243(1)	−2500	92(1)	20(1)	1
Se(11)	5784(1)	−7500	3248(1)	22(1)	1
Se(12)	7249(1)	−2500	−1475(1)	21(1)	1
Se(13)	6081(1)	−12500	5344(1)	25(1)	1
Bi(9)	7352(3)	−7500	2025(3)	25(1)	0.321(8)
K(1)	7555(5)	−7500	2358(5)	12(2)	0.540(11)
Bi(91)	7106(5)	−7500	2201(4)	22(2)	0.162(8)
Bi(8)	6998(3)	−2500	−3330(8)	26(2)	0.31(3)
K(3)	7373(6)	−2500	−3319(4)	12(2)	0.500(11)
Bi(81)	7000(3)	−2500	−3156(11)	21(2)	0.21(3)

[a] *U*(eq) is defined as one-third of the trace of the orthogonalized $\mathbf{U}_{ij}$ tensor.

Table 3. Selective Atomic Distances (Å) for the Compound $KRbBi_8Se_{13}$

Bi(1)−Se(7)	2.7304(19)	Bi(7)−Se(13)	3.1017(15)
Bi(1)−Se(3)	2.9043(14)	Bi(9)−Se(9)	2.797(3)
Bi(1)−Se(2)	3.0046(14)	Bi(9)−Se(3)	2.966(6)
Bi(2)−Se(8)	2.7326(19)	K(1)−Se(9)	3.223(7)
Bi(2)−Se(12)	2.8030(14)	K(1)−Se(7)	3.274(6)
Bi(2)−Se(2)	3.1569(14)	K(1)−Se(7)	3.274(6)
Bi(3)−Se(10)	2.7647(13)	K(1)−Se(6)	3.299(7)
Bi(3)−Se(9)	2.769(2)	K(1)−Se(3)	3.420(8)
Bi(3)−Se(3)	3.2205(15)	Bi(91)−Se(9)	2.660(4)
Bi(3)−Se(12)	3.226(2)	Bi(8)−Se(4)	2.821(6)
Bi(4)−Se(6)	2.867(2)	Bi(8)−Se(13)	2.925(14)
Bi(4)−Se(1)	2.9407(14)	K(3)−Se(4)	3.232(8)
Bi(4)−Se(5)	2.9464(14)	K(3)−Se(5)	3.235(7)
Bi(5)−Se(5)	2.797(2)	K(3)−Se(13)	3.346(10)
Bi(5)−Se(6)	2.8817(13)	K(3)−Se(8)	3.351(8)
Bi(5)−Se(13)	3.0313(14)	Bi(81)−Se(4)	2.722(7)
Bi(5)−Se(11)	3.136(2)	Bi(81)−Se(13)	3.200(18)
Bi(6)−Se(1)	2.8672(19)	Rb(2)−Se(4)	3.460(2)
Bi(6)−Se(8)	2.9450(14)	Rb(2)−Se(9)	3.476(3)
Bi(6)−Se(7)	2.9584(14)	Rb(2)−Se(10)	3.507(3)
Bi(6)−Se(2)	3.0119(18)	Rb(2)−Se(11)	3.558(3)
Bi(7)−Se(4)	2.745(2)	Rb(2)−Se(12)	3.595(3)
Bi(7)−Se(11)	2.8383(13)		

ogy, which is a common growth habit of almost all alkali metal-containing ternary and quaternary bismuth chalcogenide compounds; see Figure 1.

The lattice parameters of the $K_{2-x}Rb_xBi_8Se_{13}$ series were refined with the program U-Fit.[19] Since the larger Rb atoms substitute for K atoms, the X-ray diffraction peaks shift to lower 2θ angles as the unit cell expands. The unit cell volume increases steadily with *x* and variation approximately follows Vegard's law; see Figure 2.

Differential thermal analysis of $KRbBi_8Se_{13}$ ($x = 1$) shows one endothermic peak during heating that corresponds to melting, followed by an exothermic sharp peak of crystallization; see Figure 3. The melting points of the different members of the series were 681, 689, 682, and 682 °C for the members $x = 0.2$, 0.5, 0.8, and 1.0, respectively. However, the samples did not crystallize congruently and after the two cycles of heating/cooling both β-$K_2Bi_8Se_{13}$-type and $K_{2.5}Bi_{8.5}Se_{14}$-type phases were present.

(19) Evain, M. *U-Fit: A cell parameter refinement program*; Institut des Materiaux de Nantes: Nantes, France, 1992.

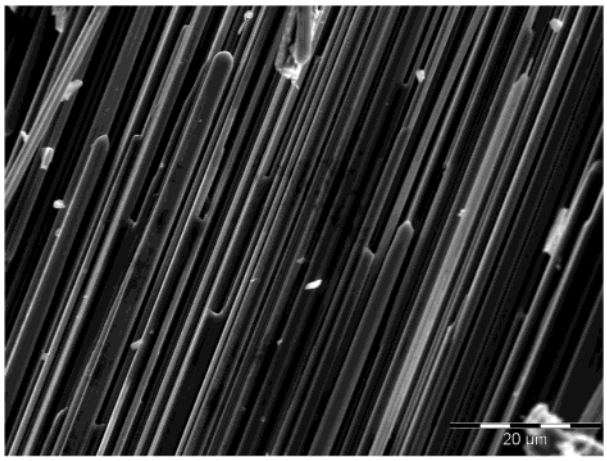

Figure 1. SEM photo of $K_{2-x}Rb_xBi_8Se_{13}$ needles ($x = 0.2$).

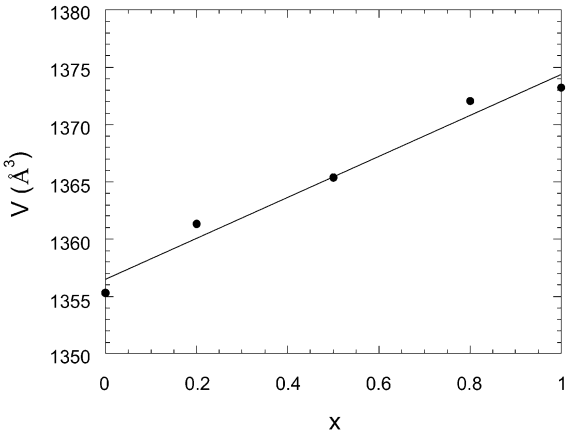

Figure 2. Unit cell volume of $K_{2-x}Rb_xBi_8Se_{13}$ versus stoichiometry *x*.

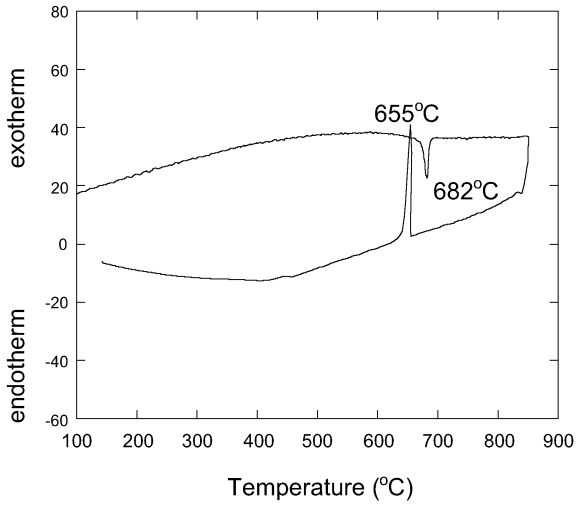

Figure 3. DTA of $KRbBi_8Se_{13}$ with a heating and cooling rate of 10 °C/min.

Structure Description. A detailed single-crystal X-ray analysis was performed on the compound $KRbBi_8$-

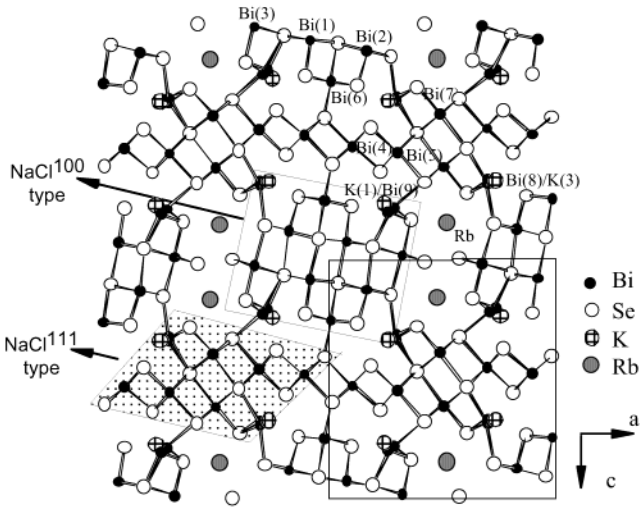

Figure 4. Crystal structure of $KRbBi_8Se_{13}$ with atom labeling.

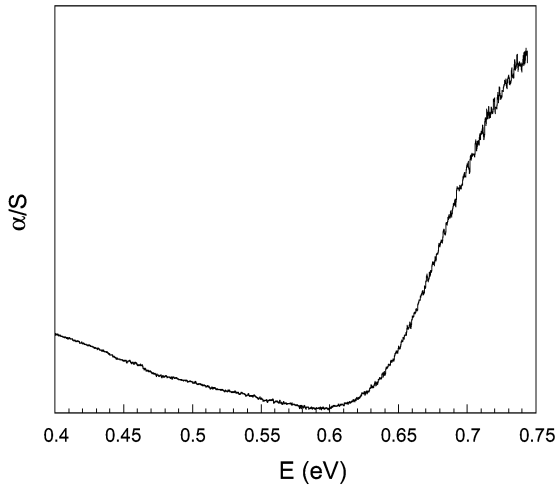

Figure 5. Infrared absorption spectrum of $KRbBi_8Se_{13}$. The band gap occurs at 0.64 eV.

Se_{13}. In this structure type, there are $NaCl^{111}$-type rods that are arranged side by side to form layers perpendicular to the *c*-axis while infinite rods of the $NaCl^{100}$-type connect the layers to build a 3-D framework; see Figure 4. The tunnels between the rods are filled with alkali metal cations. The connecting points between the two different types of blocks are disordered with Bi and K atoms. The coordination environment of the heavy metal atoms (Bi(1)−Bi(7)) is distorted octahedral with reasonable thermal parameters. The Bi−Se distances vary from 2.7304(19) to 3.226(2) Å.

In the structure of β-$K_2Bi_8Se_{13}$ there are three different crystallographic sites for the K^+ ions. One site is the so-called K(2), which is found in the centers of the tunnels. The second and third sites feature mixed occupancy with K and Bi atoms. The purpose of occupancy analysis was to examine if the Rb atom distribution is random over the K sites or if there is preferential substitution of atomic sites in the structure. In addition, we were interested to learn how the mixed K/Bi sites in the pristine material are affected by Rb^+ substitution. The gross structural model is the same as in β-$K_2Bi_8Se_{13}$, with slightly larger unit cell parameters as expected from the larger Rb atoms involved.

The Rb^+ atoms prefer exclusively the K(2) site in the spacious tunnels to the others which are the mixed occupancy sites (Bi(8)/K(3) and K(1)/Bi(9)); see Figure 4. This feature formally makes $KRbBi_8Se_{13}$ a quaternary compound that adopts the β-$K_2Bi_8Se_{13}$ structure. $KRbBi_8Se_{13}$ shows increased disorder compared to β-$K_2Bi_8Se_{13}$. The Bi(8)/K(3) site is occupied by 50.2% for K and the Bi(9)/K(1) site by 54% for K while for the K compound the occupancies are 38% and 62%, respectively.

The exclusion of Rb^+ atoms from the mixed occupancy sites is due to the larger size of the cation. Apparently Rb^+ is too big for these sites and this probably causes the different structure type of $A_2Bi_8Se_{13}$ (A: Rb, Cs).[8] On the other hand, the ability of K and Bi atoms to occupy the same crystallographic sites is probably the origin of stability of the β-$K_2Bi_8Se_{13}$ structure and of the $K_{2-x}Rb_xBi_8Se_{13}$ series (where $x \leq 1$). When $x > 1$, the β-$K_2Bi_8Se_{13}$-type cannot be adopted since any excess of Rb cannot occupy K/Bi sites. When $x \geq 1.8$, a different type of $Rb_{2-x}K_xBi_8Se_{13}$ solid solution forms, where the K atoms partially occupy the Rb sites in the $Rb_2Bi_8Se_{13}$ structure.[20]

Energy Gaps. The semiconducting energy gaps, E_g, of the members of the series were determined at room temperature using mid-infrared spectroscopy. The energy gaps clearly manifested themselves as well-defined and abrupt changes in the absorption coefficient. Band gaps of 0.6−0.61 eV were obtained for the members $x = 0.2$, 0.5, and 0.8 of the series while the band gap for $K_2Bi_8Se_{13}$ is determined[1] as 0.59 eV. Figure 5 shows the absorption spectrum of the member $x = 1$ ($KRbBi_8Se_{13}$) and its band gap at 0.64 eV. There is a small increase of band gap energy with the increase of Rb concentration in the structure. This could be attributed to the slightly more ionic nature of Rb−Se interaction and to the changes on K/Bi mixed occupation of the special sites (Bi(8)/K(3) and K(1)/Bi(9)) of the structure, which are crucial in gap formation.[3]

Thermoelectric Properties. Thermoelectric power measurements on small polycrystalline but oriented samples were carried out along the needle direction (i.e., crystallographic *b*-axis) for the $K_{2-x}Rb_xBi_8Se_{13}$ members with $x = 0.2$, 0.5 and $x = 1.0$. The Seebeck coefficient at room temperature was −179 μV/K for $x = 0.2$, −158 μV/K for $x = 0.5$, and −99 μV/K for $x = 1.0$. The Seebeck coefficient depends on the carrier concentration. In general, a decrease of thermoelectric power with composition *x* denotes the increase of carrier concentration, that is, enhancement of the n-type character of the material. The Seebeck coefficient of all members was negative and becomes less negative as the temperature is decreased down to 80 K, consistent with highly doped (i.e., degenerate) n-type semiconductors; see Figure 6a.

Electrical conductivity measurements were also carried out along the needle direction for the members of $x = 0.2$, 0.5 and $x = 1.0$. The electrical conductivity showed a weak negative temperature dependence that is consistent with semimetal or narrow-gap semiconductor behavior; see Figure 6b. The room-temperature values are 230 S/cm for $x = 0.2$, 317 S/cm for $x = 0.5$, and 730 S/cm for $x = 1.0$. Electrical conductivity tends to increase with *x* and this is consistent with the concomitant decrease of the Seebeck coefficient. This suggests a successive increase in carrier concentration with *x*.

(20) Kim, J.-H.; Kanatzidis, M. G., work in progress.

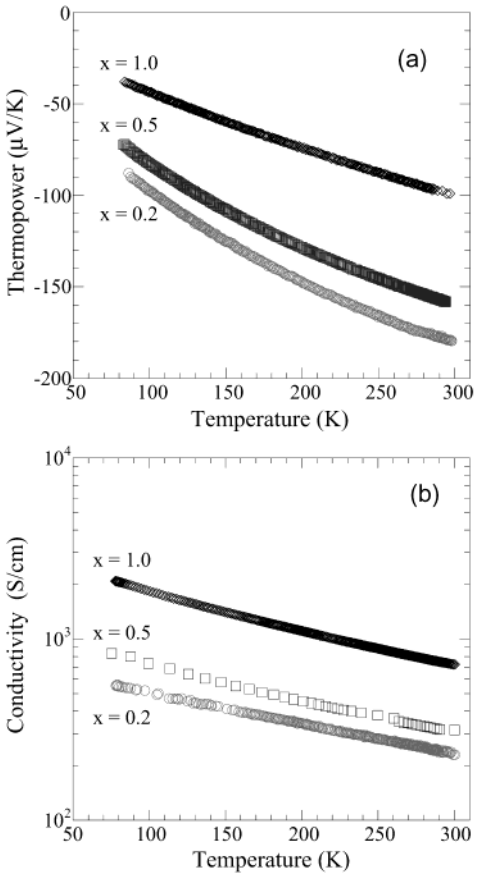

Figure 6. (a) Temperature dependence of the Seebeck coefficient for members of the $K_{2-x}Rb_xBi_8Se_{13}$ series where $x = 0.2$, 0.5, and 1.0. (b) Temperature dependence of the electrical conductivity for samples with $x = 0.2$, 0.5, and 1.0.

Hall effect measurements confirm the increase of electron concentration of the materials with composition x. The Hall coefficient (R_H) was negative for all samples and carrier concentration was calculated (based on $R_H = 1/n{\cdot}e$) to be 2×10^{19} cm^{-3} for $x = 0.2$, 4×10^{19} cm^{-3} for $x = 0.5$, and 2×10^{20} cm^{-3} for $x = 1.0$ at room temperature. The mobility (μ) was also calculated for each sample and shows a decrease with increasing x. The room-temperature values of mobility along the needle crystal axis were 74 cm^2/V·s for $x = 0.2$, 50 cm^2/V·s for $x = 0.5$, and 23 cm^2/V·s for $x = 1.0$.

To explain the observed trend of increasing carrier concentration, we need to consider the details of the crystal structure. Rb incorporation in the lattice affects only the K(2) site, which is the alkali metal site filling the tunnels of the structure. The K^+ ions incorporate into the Bi−Se framework and in fact the K/Bi distribution on the mixed occupancy sites determines the electronic properties of the material.[3] This is because the mixed occupancy sites, Bi(8)/K(3) and K(1)/Bi(9), are the connecting or disconnecting points between the two different types of building blocks in the structure. For example, when Bi occupies the site, the NaCl[111]- and NaCl[100]-type blocks are electronically connected via Bi−Se bonding whereas when K ions are present in these sites they form ionic K−Se interactions which act as "insulating" links and electronic coupling between the blocks is interrupted. These special sites therefore control the semiconducting or semimetallic behavior of the compound.[3] The Rb incorporation into the lattice affects the electronic properties of these compounds indirectly, that is, by influencing the ratio of K/Bi on the mixed sites Bi(8)/K(3) and K(1)/Bi(9) as the value of x changes. The K/Bi mixed occupancy disorder creates in-gap states that act as doping levels in these materials.[3]

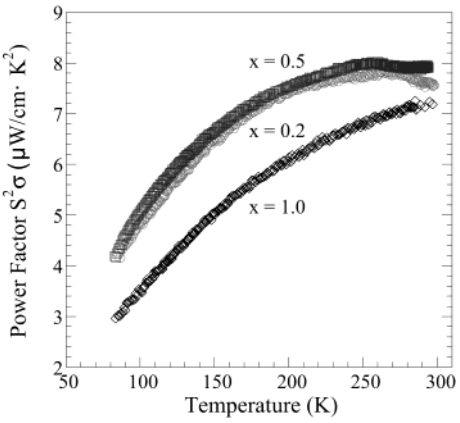

Figure 7. Power factor for samples of $K_{2-x}Rb_xBi_8Se_{13}$ with $x = 0.2$, 0.5, and 1.0.

The power factor[4] ($S^2\sigma$) was calculated for each sample and is shown in Figure 7. It increases with the temperature for all samples reaching 7.4 μW/cm·K^2 for $x = 0.2$, 7.9 μW/cm·K^2 for $x = 0.5$, and 7.2 μW/cm·K^2 for $x = 1.0$ at room temperature. These values, though lower than that of β-$K_2Bi_8Se_{13}$, which is ~12 μW/cm·K^2, are still regarded to be high when compared to most other thermoelectric materials currently under consideration.[1] The observed power factor values are much higher than those measured for the $K_2Bi_{8-x}Sb_xSe_{13}$ series.[6]

The power factor could be improved further if the mobility of the carriers could be increased. The needle-like crystal morphology of these materials affects the carrier mobility through an additional scattering mechanism. Such scattering derives from the extensive interneedle boundaries (see Figure 1) and it depends on the needle size, quality, and orientation. It can significantly reduce the carriers mobility. If the needles were large, highly oriented, and well-grown in the lateral dimensions, carrier scattering by the interneedle boundaries would be less important and the mobility would be higher. To achieve such specimens, the preparation method and the crystal growth conditions need to be optimized. Applying a crystal growth technique (e.g., Bridgman technique[21]) could result in higher quality samples and improve the carrier mobility, thus improving also the power factor.

Conclusions

The $K_{2-x}Rb_xBi_8Se_{13}$ series adopt the β-$K_2Bi_8Se_{13}$ structure type so long as $0 \le x \le 1$. The K/Rb distribution was studied in detail and strongly preferential substitution of the K sites in the tunnels of the structure was found. In other words Rb^+ displaces K^+ atoms from

(21) The Bridgman technique has been applied in various ternary and quaternary bismuth chalcogenide compounds and large and highly oriented ingots with long parallel needles were grown. Kyratsi, Th.; Chung, D.-Y.; Choi, K.-S.; Dyck, J. S.; Chen, W.; Uher, C.; Kanatzidis, M. G. *Mater. Res. Soc. Symp. Proc.* **2000**, *626*, Z8.8.1.

the tunnels and confines K^+ to the mixed Bi/K sites in the Bi/Se framework. Rb itself is excluded from those sites due to its large size. At $x = 1$ the resulting $KRbBi_8Se_{13}$ is best described as a quaternary compound. All members are n-type semiconductors with increasing carrier concentration as a function of x. This is attributed to increased K/Bi disorder in the special mixed occupancy sites of the β-$K_2Bi_8Se_{13}$ structure that increases the number of mid-gap levels. The work described here, and previous results on $K_2Bi_8Se_{13}$ and the solid solutions $K_2Bi_{8-x}Sb_xSe_{13}$, place increased emphasis on the mixed K/Bi sites and the critical role they play in regulating the charge transport properties of these materials. Gaining control of these sites could hold the key in optimizing the thermoelectric properties in these systems.

Acknowledgment. We thank Dr. P. N. Trikalitis for his help with the SEM photos and for financial support the Office of Naval Research (Contract No. N00014-02-1-0867). Work at NU also made use of the Central Facilities supported by the National Science Foundation through the Materials Research Center (DMR-0076097).

Supporting Information Available: Crystallographic information (CIF). This material is available free of charge via the Internet at http://pubs.acs.org.

CM034185V